J. Fluid Mech. (2002), *vol.* 454, *pp.* 403–417. © 2002 Cambridge University Press 403
DOI: 10.1017/S0022112001007200 Printed in the United Kingdom

Do true elevation gravity–capillary solitary waves exist? A numerical investigation

By A. R. CHAMPNEYS[1], J.-M. VANDEN-BROECK[2] AND G. J. LORD[3]

[1]Department of Engineering Mathematics, University of Bristol, BS8 1TR, UK
a.r.champneys@bristol.ac.uk,

[2]School of Mathematics, University of East Anglia, Norwich NR4 7TJ, UK
J.Vanden-broeck@uea.ac.uk

[3]Department of Mathematics, Heriot-Watt University, Edinburgh EH14 4AS, UK
gabriel@ma.hw.ac.uk

(Received 18 December 2000 and in revised form 13 July 2001)

This paper extends the numerical results of Hunter & Vanden-Broeck (1983) and Vanden-Broeck (1991) which were concerned with studies of solitary waves on the surface of fluids of finite depth under the action of gravity and surface tension. The aim of this paper is to answer the question of whether small-amplitude elevation solitary waves exist. Several analytical results have proved that bifurcating from Froude number $F = 1$, for Bond number τ between 0 and 1/3, there are families of 'generalized' solitary waves with periodic tails whose minimum amplitude is an exponentially small function of $F-1$. An open problem (which, for τ sufficiently close to 1/3, was recently proved by Sun 1999 to be false) is whether this amplitude can ever be zero, which would give a truly localized solitary wave.

The problem is first addressed in terms of model equations taking the form of generalized fifth-order KdV equations, where it is demonstrated that if such a zero-tail-amplitude solution occurs, it does so along codimension-one lines in the parameter plane. Moreover, along solution paths of generalized solitary waves a topological distinction is found between cases where the tail does vanish and those where it does not. This motivates a new set of numerical results for the full problem, formulated using a boundary integral method, namely to probe the size of the tail amplitude as τ varies for fixed $F > 1$. The strong conclusion from the numerical results is that true solitary waves of elevation do not exist for the steady gravity–capillary water wave problem, at least for $9/50 < \tau < 1/3$. This finding confirms and explains previous asymptotic results by Yang & Akylas.

1. Introduction

The description of wave propagation under the combined effects of gravity and surface tension on the surface of a liquid above a horizontal bottom is a classical problem in applied mathematics with a long history (Korteweg & de Vries 1895; Wilton 1915). In the last twenty years or so there have been a number of advances in the understanding of this problem, using a variety of numerical, asymptotic and rigorous analytical methods (see the review by Dias & Kharif 1999). We focus exclusively on two-dimensional steady waves. For solitary waves, the problem can be characterized by the Froude number F and the Bond number τ defined by

$$\tau = T/\rho g H^2, \quad F = c/\sqrt{gH}, \tag{1.1}$$

Here, g is the acceleration due to gravity, T is the coefficient of surface tension, ρ is the density of the fluid, H is its depth and c is the propagation speed of the wave.

When $\tau > 1/3$, given values of $F < 1$ in an appropriate range, it is known that there are isolated solitary waves of depression (with a negative central crest) both via existence theory (Amick & Kirchgassner 1989; Iooss & Kirchgassner 1992; Buffoni, Groves & Toland 1996) and numerical computation (Hunter & Vanden-Broeck 1983; Dias, Menasce & Vanden-Broeck 1996). We mention that for certain F-values these predominantly depression waves develop decaying oscillatory tails, and that near the minimum of the dispersion curve for gravity–capillary waves these become envelope waves, some of which have positive central crests. In what follows we shall draw a distinction between these envelope waves and genuine *waves of elevation* which have a large positive crest without being surrounded by other peaks and troughs of comparable amplitude. Indeed for $\tau < 1/3$, and fixed values of $F > 1$, it is known that there are steady solutions which form one-parameter families of such elevation waves. They are not, however, true *solitary* waves, but are instead characterized by a train of ripples of constant amplitude in the far field (Beale 1991; Sun 1991). These are called *generalized solitary waves*, to distinguish them from true solitary waves which are characterized by an asymptotically flat free surface at large distance from the core.

The ripples in the tail of the generalized solitary waves are of questionable physical validity because they occur on both sides and therefore do not satisfy radiation conditions without the supply of energy from infinity. Therefore an important question is whether the free parameter can be chosen so that the amplitude of the ripples vanishes. One of the key known features of these ripples is that the amplitude is an exponentially small function of $F - 1$, as has been shown both by exponential asymptotics (Sun & Shen 1993) and by rigorous application of centre manifold and normal form theory (Lombardi 2000). Lombardi's analysis (see also the discussion in § 3 below) also suggests that for fixed $\tau < 1/3$, it is non-generic that zero-tail-amplitude solutions bifurcate from $F = 1$. What is not known is whether there are isolated τ values less than 1/3 at which such true solitary waves bifurcate. This question has been rigorously answered in the negative for τ sufficiently close to 1/3 by Sun (1999). The aim of this paper is to numerically probe the question of whether true solitary waves bifurcate for general $\tau < 1/3$. A key previous result in this direction is that of Yang & Akylas (1996) who use complex-time asymptotics to estimate the 'beyond all orders' amplitude of the periodic tail as $F \to 1$. They conclude for seven discrete values of τ that this tail amplitude is not zero, and the general trend is that the constant multiplying the exponentially small term varies monotonically with τ. The validity of the asymptotics is also backed up in that work by numerical results using a spectral method valid for small tail amplitude, but only for the fixed value $\tau = 0.3$. Related numerical and asymptotic results are also known for interfacial and internal solitary waves (Akylas & Grimshaw 1992; Michallet & Dias 1999).

The numerical method we use is not restricted to generalized solitary waves with small amplitude. Hence we are able to probe the topological structure of solution branches of generalized solitary waves, which will lead us to an important observation about the structure of models which possess true elevation waves, compared with those which do not. Specifically, we approximate solitary waves by periodic waves of sufficiently long period and solve the full nonlinear equations for water waves by a boundary integral method. Hunter & Vanden-Broeck (1983) were the first to compute generalized solitary waves in this way. Later, in Vanden-Broeck (1991), it was shown for a fixed τ-value, that the amplitude of the ripples computed can be minimized so that they are invisible on the scale of the waves. Here we present extended calculations to explore whether or not this minimum amplitude is really zero. In order to do this we appeal to intuition gained from first studying an extended fifth-order Korteweg–de Vries model (5thKdV) equation.

The results are presented as follows. In § 2 we recall briefly a formulation of the classical water wave problem we study and how it has been approximated by various KdV-type model equations. Section 3 then presents a series of numerical experiments on two different forms of the extended 5thKdV equation. The parameter dependence of generalized solitary waves is uncovered both in a case when the tails do vanish and when they do not. Section 4 then introduces the numerical method to be used for the full problem and, taking insight from the results in § 3, presents a set of numerical experiments specifically designed to probe the minimum size of the tail amplitude of the generalized solitary waves. Finally, § 5 draws conclusions.

2. Formulation

We consider a train of periodic waves of wavelength L travelling at a constant velocity C at the surface of a two-dimensional fluid of finite depth H. The fluid is assumed to be inviscid and incompressible, and the flow to be irrotational. In particular we define a velocity potential ϕ and stream function ψ and choose $\phi = 0$ at a crest and $\psi = 0$ on the free surface. Gravity g and surface tension T are both taken into account. The velocity C is defined as the average horizontal fluid velocity at any horizontal level completely within the fluid. The depth H is defined by $H = Q/C$ where Q is the value of $|\psi|$ on the bottom. Solitary waves are defined by taking the limit $L/H \to \infty$. Numerically they will be approximated by periodic waves with large L/H (typically ~ 100). We henceforth non-dimensionalize by setting $H = C = 1$ and introducing the dimensionless Froude number F and Bond number τ defined in (1.1). We use a coordinate system with x horizontal and y measured vertically upwards from the horizontal bottom.

This problem can be formulated in terms of potential flow with nonlinear dynamic and kinematic boundary conditions on the free surface (e.g. Stoker 1957). It can also be reformulated as a system of integro–differential equations for the x and y coordinates of a material point on the fluid surface as a function of the complex potential function $f = \phi + \mathrm{i}\psi$ where $\psi = 0$ defines the free surface. We restrict our attention to waves which are symmetric with respect to $\phi = 0$. Using a Cauchy integral formula we obtain (Vanden-Broeck & Schwartz 1979; Hunter & Vanden-Broeck 1983; Vanden-Broeck 1991)

$$\begin{aligned} x'(\phi) - 1 = &-\frac{1}{L}\int_0^{L/2} y'(s)\left(\cot\frac{\pi(s-\phi)}{L} + \cot\frac{\pi(s+\phi)}{L}\right)\mathrm{d}s \\ &+\frac{2r_0}{L}\int_0^{L/2}\frac{[x'(s)-1]\{r_0^2 - \cos[(2\pi/L)(s-\phi)]\} - y'(s)\sin[(2\pi/L)(s-\phi)]}{1 + r_0^4 - 2r_0^2\cos[(2\pi/L)(s-\phi)]}\mathrm{d}s \\ &+\frac{2r_0}{L}\int_0^{L/2}\frac{[x'(s)-1]\{r_0^2 - \cos[(2\pi/L)(s+\phi)]\} - y'(s)\sin[(2\pi/L)(s+\phi)]}{1 + r_0^4 - 2r_0^2\cos[(2\pi/L)(s+\phi)]}\mathrm{d}s, \end{aligned} \tag{2.1}$$

$$\frac{F^2}{2}\left(\frac{1}{x'(\phi)^2+y'(\phi)^2}-1\right)+y+\tau\frac{x'(\phi)y''(\phi)-x''(\phi)y'(\phi)}{[x'(\phi)^2+y'(\phi)^2]^{3/2}}=0, \tag{2.2}$$

where F is the Froude number and

$$r_0 = \mathrm{e}^{-2\pi/L}.$$

This latter formulation will be adopted below since it is more convenient for numerics as mesh points are only required to be stationed on the free surface rather than throughout the fluid domain.

In the limit $F \to 1$, the waves are of small amplitude. Therefore solutions may be described by weakly nonlinear theories. To derive them, we move to a steady frame and denote the equation for the free surface as $y = H + A\eta$. Here A is a parameter measuring the amplitude of the wave. For small A, $\eta(x)$ satisfies the KdV equation

$$2(F-1)\eta' - 3\eta\eta' + (\tau - \tfrac{1}{3})\eta''' = 0 \tag{2.3}$$

(see Korteweg & de Vries 1895 for a derivation). This equation has periodic travelling solutions (cnoidal waves) which tend in the limit of long wavelength to the famous solitary wave solution described by the function sech^2. This describes a depression wave for $\tau > 1/3$, $F < 1$ and an elevation wave for $\tau < 1/3$, $F > 1$.

When $\tau = 1/3$, the dispersive term in (2.3) vanishes and hence there are no periodic or solitary wave solutions. As $\tau \to 1/3$, the appropriate long-wave equation is the fifth-order KdV equation (5thKdV) also known as the Kawahara equation

$$2(F-1)\eta' - 3\eta\eta' + (\tau - \tfrac{1}{3})\eta''' - \tfrac{1}{45}\eta^{(5)} = 0, \tag{2.4}$$

which may be derived by a regular asymptotic expansion near $\tau = 1/3$, $F = 1$ (Hunter & Vanden-Broeck 1983, § 2). There are other derivations of this equation, with different coefficients, in several other physical contexts (e.g. Kakutani & Ono 1969; Hasimoto 1970; Kawahara 1972; Zufiria 1987; Hunter & Scheurle 1988; Karpman 1994). The properties of its solutions are discussed in § 3 which follows. Also, equations have been derived with extra nonlinear terms, see Kichenassamy & Olver (1996) and references therein. It is precisely such a model that we study in the § 3. The values of the parameters we take there are not necessarily ones in which the 5thKdV is a good approximation of the full water-wave problem. Instead, we merely treat the model as a guide of what to expect qualitatively when studying the full model numerically.

3. Solitary waves of fifth-order KdV equations

In Champneys & Groves (1997) the following extended 5KdV model for the free surface $u(x)$ of the capillary–gravity water-wave problem was considered:

$$u_t + \tfrac{2}{15}u_{xxxx} - bu_{xxx} + 3uu_x + \mu[u_x u_{xx} + uu_{xxx}] = 0 \tag{3.1}$$

It reduces to the fourth-order ODE

$$\tfrac{2}{15}u'''' - bu'' + au + \tfrac{3}{2}u^2 + \mu[(uu')' - \tfrac{3}{2}(u')^2] = 0 \tag{3.2}$$

upon moving to a steady frame moving at speed a and integrating once, choosing the integration constant to be zero in order to describe solitary waves. This model may be derived using Hamiltonian perturbation theory from the full water-wave problem (Craig & Groves 1994), and is a special case of the more general form studied by Kichenassamy & Olver (1996). The parameters a and b are related to the Froude and

Bond numbers via

$$\frac{a}{2} = \frac{1}{F} - 1, \quad b = \frac{\tau - 1/3}{F^2}.$$

Hence as $\tau \to 1/3$ and $F \to 1$ the parameters a and b play the roles of the difference of Froude and Bond numbers respectively from the critical codimension-two point. Specifically we have the scalings

$$a \sim -2(F-1), \quad b \sim \tau - \tfrac{1}{3} \quad \text{for} \quad F \sim 1, \quad \tau \sim \tfrac{1}{3}.$$

Finally, μ is an artificial parameter that represents the relative importance of various nonlinear terms in the long-wave expansion. Only its sign is important, since non-zero μ can be rescaled to unity; here we study only $\mu = 0$ or 1. The case $\mu = 0$ gives (a scaling of) the usual 5thKdV equation (2.4). An overview of parameter space may be found in Champneys & Groves (1997). Two parameter regions are of interest: $a > 0$ and $a < 0$, and we discuss these below for both $\mu = 0$ and $\mu = 1$.

Essentially, with $a > 0$ solitary wave solutions are all waves of depression, which tend to envelope solitary waves in the limit of small amplitude as b is decreased to $-\sqrt{8a/15}$. In fact there are also infinitely many multi-troughed 'bound state' versions of these solutions for $-\sqrt{8a/15} < b < \sqrt{8a/15}$ some of which are stable as a solution of the evolutionary problem (see Buffoni, Champneys & Toland 1996; Buffoni & Séré 1996; Yang & Akylas 1997; Buryak & Champneys 1997; Dias & Kuznetsov 1999; Calvo, Yang & Akylas 2000; Bridges & Derks 1999) for recent rigorous, asymptotic and numerical results. In another limit, $a \to 0^+$ for $b > 0$, a unique solitary wave solution bifurcates at zero amplitude, in so doing tending to the soliton solution of the usual third-order KdV equation, which can be recovered in this limit after rescaling. Many of these results for $a > 0$ extend to the case $\mu > 0$ and can also be shown to have rigorous implications via spatial centre-manifold reduction, for the existence of qualitatively similar solutions for the full water-wave problem.

The existence of solitary wave solutions for $a < 0$ is much more subtle and forms the subject of this paper. Essentially, the limit $a \to 0^-$ for $b < 0$ also captures the usual third-order KdV equation after rescaling (as did the limit $a \to 0^+$, $b > 0$). The perturbation that the 5thKdV adds to the soliton solution of the KdV equation (which is a wave of elevation in this case) is a rapid oscillatory term. This then is a beyond-all-orders asymptotics problem and has been studied by many authors (e.g. Pomeau, Ramani & Grammaticos 1988; Amick & Toland 1992; Grimshaw & Joshi 1995; Sun 1998). Recent rigorous theory by Lombardi (2000) for a class of systems including (3.2) is the most comprehensive. He shows that generically in the limit of $a \to 0$ there do not exist true solitary waves of elevation, but there are one-parameter families of generalized solitary waves, which represent homoclinic connections between periodic orbits, the minimum amplitude of which is an exponentially small function of a as $a \to 0$. For (3.2) with $\mu = 0$, it is known that there are no true solitary waves as $a \to 0$ (Amick & McLeod 1991), that is the tail amplitude never vanishes. Also, the family of generalized solitary waves (for fixed a and b) traces a 'u-shaped' locus in a plot of amplitude of tail vs. phase shift between tails (Grimshaw & Joshi 1995). This locus has a slight asymmetry as was first spotted numerically (Champneys & Lord 1997) and then confirmed analytically (Sun 1998), see for example one of the u-shaped curves in figure 1(a).

The case $\mu = 1$ is very different, since there is an explicit true solitary wave solution that exists along the line

$$a = \tfrac{3}{5}(2b+1)(b-2), b \geqslant -\tfrac{1}{2}, \quad u(x) = 3(b + \tfrac{1}{2})\operatorname{sech}^2\left(\sqrt{\frac{3(2b+1)}{4}}x\right). \tag{3.3}$$

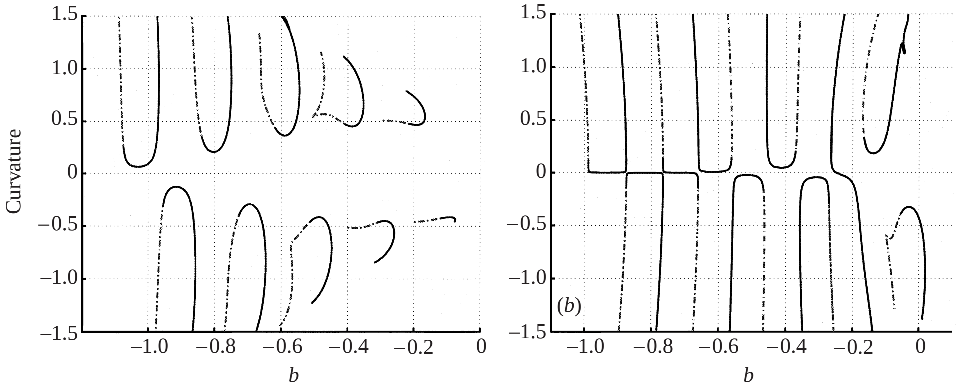

FIGURE 1. Solution loci of long-periodic approximations to generalized solitary waves of the 5thKdV model (3.2) with $a = -0.675$. Here a signed measure of the tail amplitude, namely the curvature of the right-hand end-point of the wave computed with symmetric boundary conditions on an interval $L = 43.2$, is plotted against Bond number b. Panels (a) and (b) contrast the cases $\mu = 0$ and $\mu = 1$ respectively. Solid lines correspond to a local maximum at the central crest of the wave, and dot-dashed lines to a local minimum. Note that the zero-curvature solutions in (b) correspond to true elevation solitary waves.

Numerically, Champneys & Groves (1997) found this to be the first among a countable number of branches that bifurcate at small amplitude from $a = 0^-$ for smaller values of $b < 0$. (Where these branches cross $a = 0$, for $b > 0$ – e.g. at $b = 2$ for the explicit solution (3.3) – does not correspond to a bifurcation, because the wave has finite amplitude there, but corresponds to the wave becoming a codimension-one 'orbit flip' bifurcation of generic solitary waves; see Champneys & Groves 1997.) In Champneys (2000) many other fourth-order model systems are studied, and it is found that there are many other cases when such 'persistence' of true solitary wave solutions from the singular limit occur. Note that this is not in contradiction with Lombardi's proof of generic non-persistence, since the solitary waves occur only along lines in a parameter plane. In fact a straightforward argument counting dimensions of stable and unstable manifolds of the fourth-order ODE (3.2) shows that, if solitary waves solutions occur, then they should be of codimension one in parameter space, provided that their profiles are even (non-symmetric waves are of codimension two).

The purpose of the new results presented in this section is to see how the persistence or non-persistence of true solitary waves affects the global structure of the generalized solitary wave solutions to the 5thKdV equation. Later on, we adapt this insight to draw conclusions based on our numerical findings for the full water-wave problem. Some results for fixed $a = -0.675$ are presented in figures 1–5. Before discussing the results, let us briefly mention the method by which they were obtained, which, in order for a closer analogy to be drawn with results for the full water-wave problem, is rather simpler than that used in our earlier work (Champneys & Lord 1997) (nevertheless, almost identical results have been obtained using the method used in that work). The generalized solitary waves are approximated by a periodic orbit of a fixed long period $-L/2 < x < L/2$ ($L = 43.2$ for the results presented), where periodicity in this time-reversible system is guaranteed by taking boundary conditions $u'(-L/2) = u'''(-L/2) = u'(L/2) = u'''(L/2) = 0$. For each fixed a and b parameter value, this then fixes the phase shift between the tails. We then perform numerical continuation on this periodic boundary-value problem using AUTO (Doedel *et al.* 1997) for fixed a, allowing b to vary. This is motivated by the fact that computation

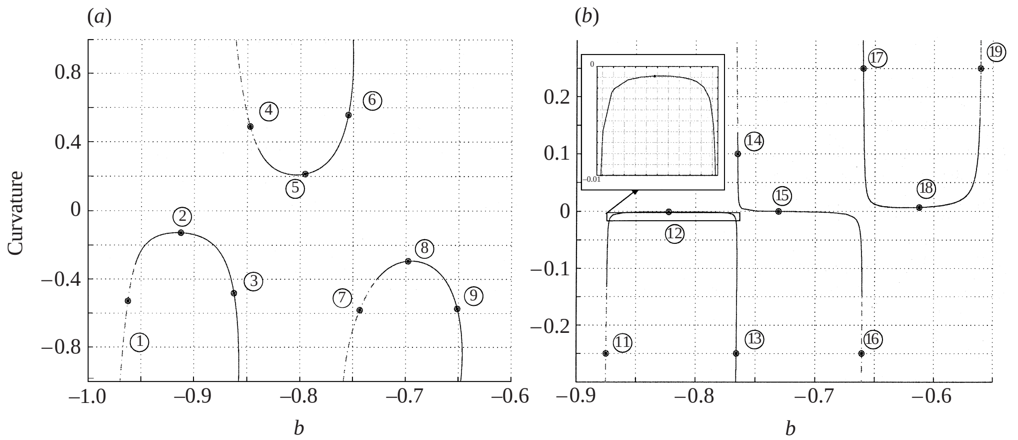

FIGURE 2. Details of figure 1; (a) for $\mu = 0$, and (b) for $\mu = 1$. The point numbers refer to the solutions shown in figures 4 and 5. The inset on (b) shows that the leftmost n-shaped curve is bounded away from zero curvature.

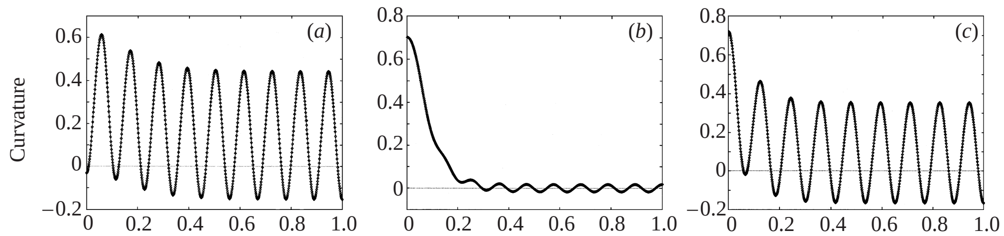

FIGURE 3. Global structure of the solutions on the middle (upper) branch of figure 2(a) for ($\mu = 0$). These solutions are at b-values −0.894, −0.794 and −0.770 for (a)–(c), which correspond to respective end-curvature values 2.09, 0.21 and 1.64. Only the right-hand portion of the wave from its point of symmetry is depicted, and the horizontal scale has been divided by a factor $L/2 = 21.6$.

into the singular limit $a \to 0$ is undesirable, and by the observation from the model equations in Champneys (2000) that curves of true solitary wave solutions bifurcate from $a = 0$ at a non-zero angle. Now, this one-parameter sweep is therefore just a slice through a three-parameter surface parametrized by phase shift (effectively L) and the model parameters a and b. Hence it would seem possible that we might miss curves in the (a, b)-plane corresponding to true solitary waves. However, if a true solitary wave is found then by definition the phase shift between the zero solution at $x = -\infty$ and $x = +\infty$ is not defined, and hence computing with *any fixed phase shift* will find (a good numerical approximation to) this homoclinic solution. Indeed, this is precisely what we found by performing calculations with different L-values. Finally, we simplify the problem by looking only for symmetric solutions (with the first two boundary conditions replaced by $u'(0) = u'''(0) = 0$) and as a measure of the amplitude of the tail we take the curvature of the right-hand boundary point $u''(L/2)$. Using curvature in this way has the advantage that it is a signed quantity, which is helpful for qualitative interpretation of the results.

Let us now compare the results presented for $\mu = 0$ and $\mu = 1$. Consider first $\mu = 0$, figures 1(a), 2(a), 3 and 4. Here the generalized solitary waves lie on a succession of disconnected, alternating ‘u’- and ‘n-shaped’ curves. At the local minimum or maximum of each curve is the minimum-tail-amplitude solution. Note that taking

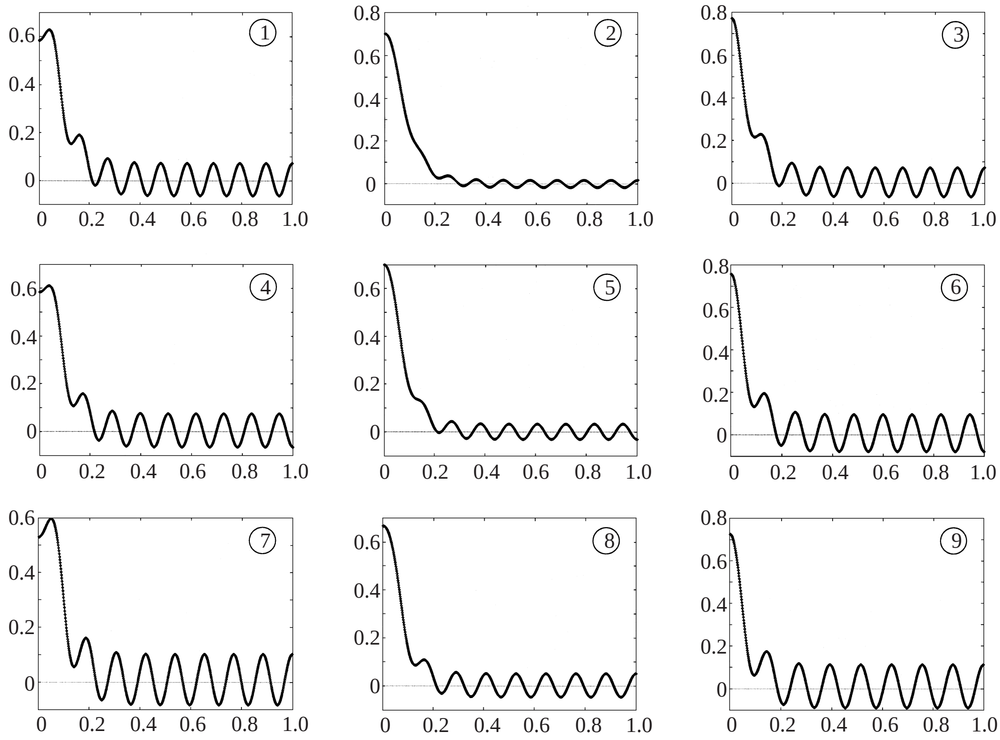

FIGURE 4. Structure of the solutions on the three branches shown in figure 2(*a*) ($\mu = 0$). Only the right-hand portion of the wave from its point of symmetry is depicted, and the horizontal scale has been divided by a factor $L/2 = 21.6$. Note that the central core is at a minimum for solutions at labels 1, 4 and 7 as indicated by the dashed portion of the curves in figure 2.

this sweep in b is similar to taking a sweep in L for fixed b and a because, since the period of the tail depends on b, then both b and L effectively control the phase shift between the two tails. The structure of solutions on each u or n is qualitatively similar, with the large-curvature limit of all branches representing a localized modulation of a large-amplitude, pure periodic wave (see figure 3). Note that the numerical continuation of several branches for τ close to $1/3$ (whose graphs end in 'mid air' in figure 1(*a*)) was halted because the global shape of the branch became more complicated, and there was evidence that the solution was beginning to be influenced by the finiteness of L.

The situation for $\mu = 1$ is qualitatively different, see figures 1(*b*), 2(*b*) and 5. Here, in addition to u- and n- there are also 's-shaped' curves where the tail amplitude goes through zero. Two such zero-tail-amplitude points are detected in figure 1(*b*) – the first of these is at precisely the value $b = -0.25$ given by the formula (3.3); the neighbourhood of the second one is blown up in figure 2(*b*) and occurs at a value of $b \approx -0.7307924$. This shows how true solitary wave solutions are embedded into loci of generalized solitary waves. That is, there is a topological difference between the cases where true solitary waves occur and those where they do not. Namely, true solitary waves lie on s-shaped curves. This is significant, since rather than have to carefully check the size of something that is exponentially small in a, we have produced a numerical criterion for deciding whether true solitary waves exist which relies on computing $O(1)$ quantities. The criterion is simply that true solitary waves exist when there are s-shaped curves.

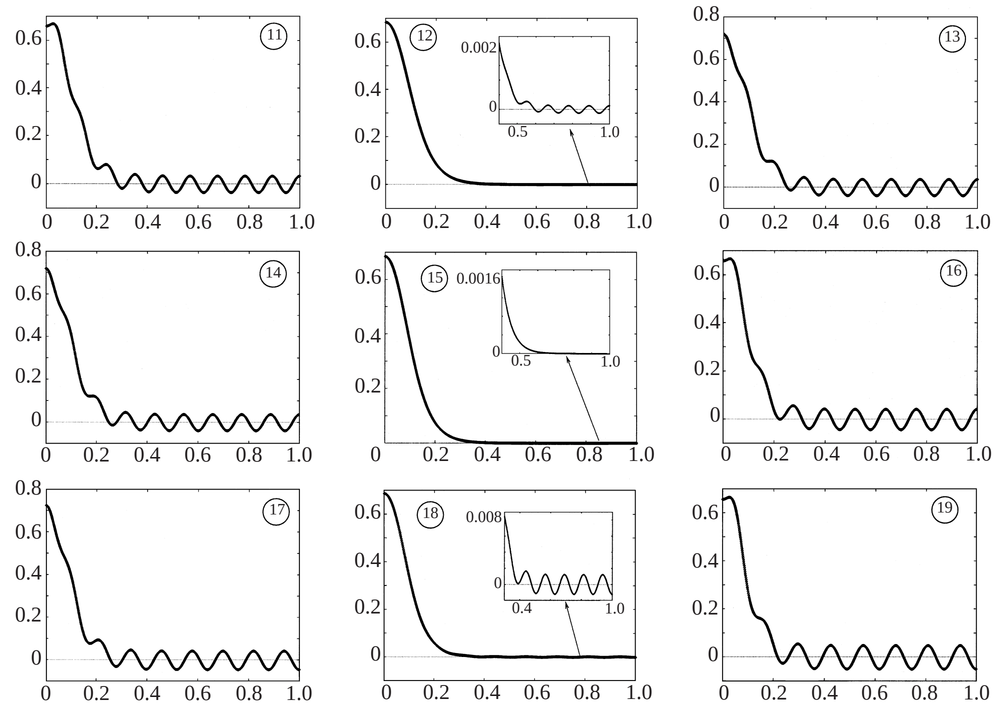

FIGURE 5. Structure of the solutions on three branches shown in figure 2(*b*) ($\mu = 1$), plotted on the same horizontal scale as in figure 4. Insets in the middle three panels show the detail of the tail of the wave at the three points close to zero end curvature. Only point 15 is a true solitary wave.

Note that any attempt to continue the zero-curvature solutions on the s-shaped curves in figure 1(*b*) from $\mu = 1$ to $\mu = 0$ resulted in solution curves in the (b, μ)-plane that move to $b = -\infty$ as $\mu \to 0$. This is again strong evidence that no true elevation solitary wave solution exists for $\mu = 0$.

4. Numerical results for the exact water wave problem

Our numerical procedure for solving (2.1), (2.2) follows closely the boundary integral method used by Hunter & Vanden-Broeck (1983) and Vanden-Broeck (1991), to which the reader is referred for the details. We approximate (generalized) solitary waves by long, even, periodic waves of wavelength L. This approximation enables us to overcome difficulties associated with the appropriate choice of boundary conditions in the far field. As $L \to \infty$, the periodic waves approach generalized solitary waves (for a numerical study of this limit, see Vanden-Broeck 1997). The solutions are described in terms of four parameters. A solution is defined by fixing the values of three of these parameters (the value of the fourth comes as part of the solution). There are different convenient choices for the four parameters. The first three are L (or equivalently r_0), τ and F. In Vanden-Broeck (1991), the fourth parameter was defined as the velocity of the crest. This is a measure of the wave amplitude, in the sense that when this parameter is close to one, the wave is of small amplitude. In this work we find it more convenient to choose this additional free parameter to be the curvature at the trough of the wave, as this is a measure of the amplitude of the ripples in the tail. Moreover, as illustrated for the 5thKdV models in the previous

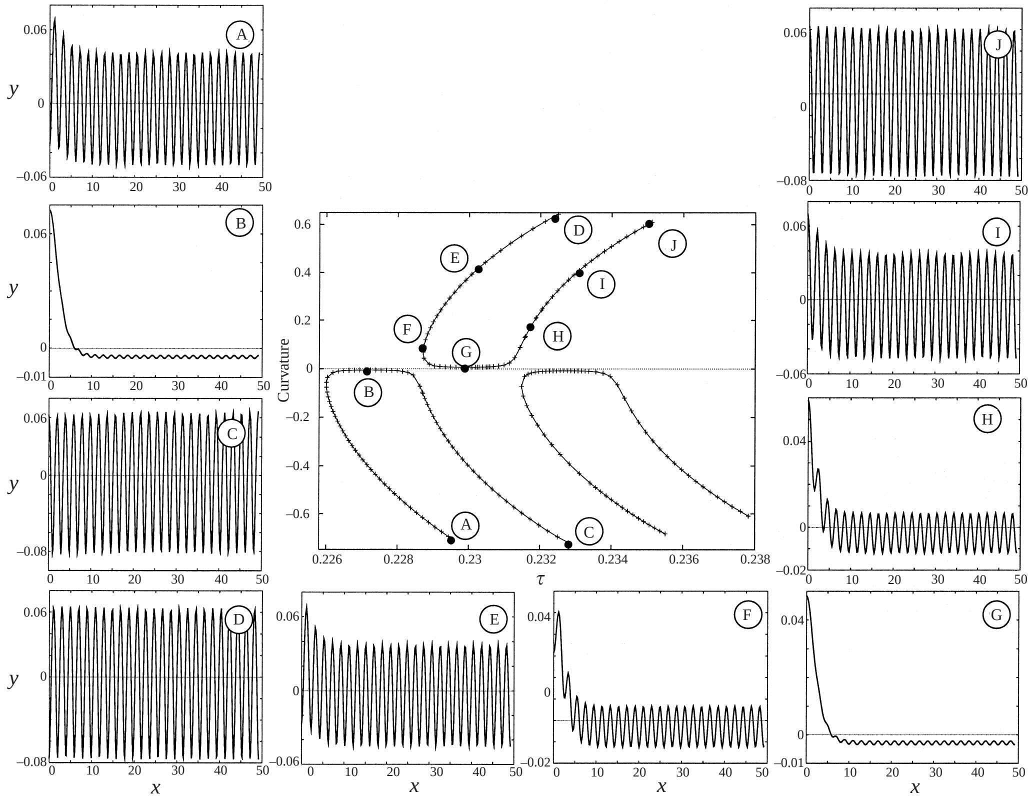

FIGURE 6. Illustrating the global structure of solution branches for a consecutive sequence of three branches for $F = 1.02$, $L = 98.33$ and $0.226 < \tau < 0.238$, computed with $N = 269$. Panels A–J depict for the upper branch the detailed profiles of the free surface, illustrating the transitions that take place as the u-shaped curve is traversed. Solutions at three points on the left-hand n-shaped curve are also presented.

section, the curvature is a signed quantity which can be used to extract the topological information of whether solutions lie on purely u- and n-shaped curves, or whether they are interspersed with s-shaped ones. Practically, this curvature is measured using a second-difference formula at the right-hand end-point of the free surface.

The system (2.1), (2.2) is discretized by following the procedure described in Hunter & Vanden-Broeck (1983) and Vanden-Broeck (1991), with the resulting set of nonlinear algebraic equations solved by Newton's method. Error tolerances were typically set at 10^{-7}. The accuracy of solutions was found to be highly dependent on the number of mesh points N used. Solution loci of tail curvature versus τ were computed using simple natural parameter continuation in either τ or the curvature.

Figure 6 presents some results for fixed F and L with $N = 269$. Three successive branches of solutions are plotted as tail curvature vs. τ. Panels A–J show the free surface profiles. Note the striking similarity between the structure of solutions found on the u- and n-shaped curves here and those for the 5thKdV results in figures 1–4. Each solution locus connects two end-points corresponding to pure-periodic waves with opposite phases at the central point. In between these large-amplitude extremes is a portion of the locus where the waves have small tail amplitude.

Figures 7 and 8 motivate the choice of F and L taken in these computations.

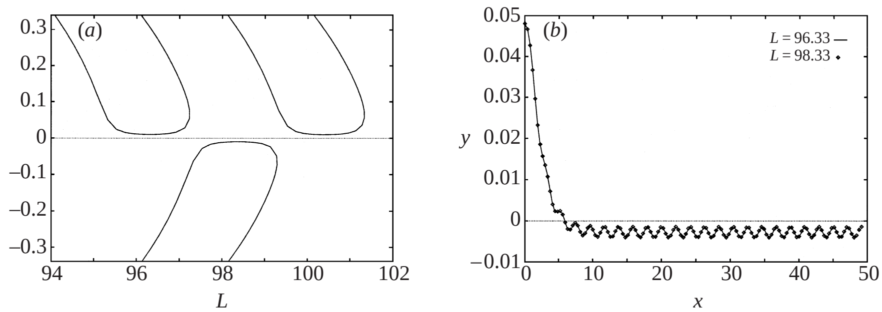

FIGURE 7. The dependence on the length L: (a) shows the results of continuation in L for fixed Bond and Froude numbers $\tau = 0.239462$ and $F = 1.02$; (b) compares the solutions at approximately the minimum of curvature for the two successive positive branches. Note that the two solutions are overlaid at the scale depicted.

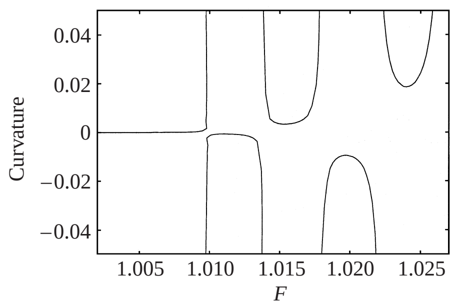

FIGURE 8. The dependence on the Froude number F for fixed $L = 98.33$, $\tau = 0.239462$. Only the small-curvature parts of the branches are depicted. Note that the minimum curvatures on branches for $F < 1.01$ are smaller than the numerical accuracy.

Changing L (keeping τ and F fixed) results in a periodic sequence of identical u- and n-shaped curves which correspond to longer and longer approximations to the same family of generalized solitary waves. Decreasing the Froude number further towards the critical value $F = 1$ (keeping τ and L fixed) again creates sequences of u and n shapes but they become increasingly square, that is the tail amplitude becomes negligible for large portions of the solution locus, separated by almost vertical walls of rapid growth in tail amplitude at almost constant F. For $F < 1.01$, for the τ-value chosen, the size of the tail amplitude was found to be commensurate with error tolerances used in Newton's method and the vertical walls become hard to detect numerically. The rest of the computations presented use the fixed values $L = 98.33$ and $F = 1.02$.

Figure 9 presents results on the convergence of solutions with variation of the number of mesh points N. It compares results for three different values of τ. Panels (a) and (b) illustrate that increasing the number of mesh points from those used for the results in figure 6 makes little quantitative difference, suggesting that the mesh has effectively converged. Taking a smaller mesh, even as drastically as halving the number of mesh points, makes a difference in the third decimal for τ, but (crucially) only in the fourth or fifth decimal place for the minimum value of the end curvature. Note also that the agreement becomes better as τ increases (see panels c and d). So while taking a mesh of $N = 269$ is desirable for accurately reproducing solutions at a given τ-value, it seems that $N = 135$ is sufficient for unfolding the global topology of

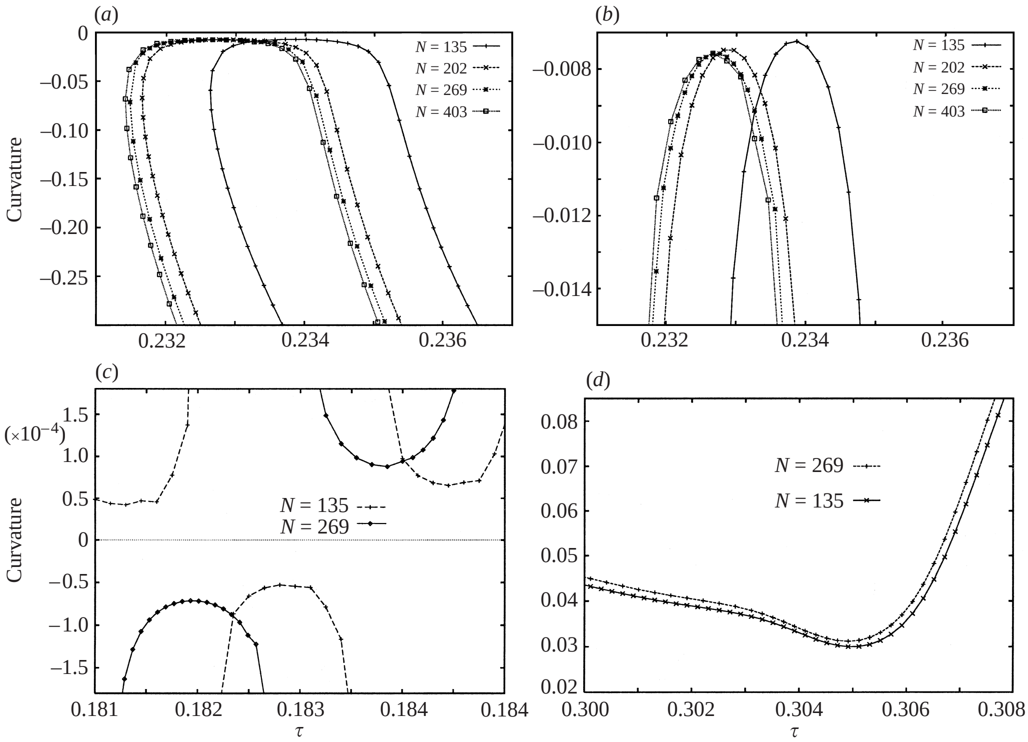

FIGURE 9. Illustrating the dependence on the number of mesh points N for $L = 98.33$ and $F = 1.02$. (*a*) Results for four different N-values plotted for one particular branch for $0.231 < \tau < 0.237$, a zoom of the small curvature end of which is depicted in (*b*). (*c, d*) Similar comparisons between two N-values, for the small-curvature tip of branches for two different values of τ.

the solution set. This latter value is also more practical since the typical time taken for Newton's method to converge to one solution point is the order of 500 s (on a SUN SPARC 10), compared with about 5000 s for $N = 269$.

Finally then, figure 10 presents the results of a global sweep of $\tau < 1/3$. For the given Froude number, computation for $\tau < 0.18 = 9/50$ was impractical, since the size of the minimum tail amplitude became comparable with the error tolerance in Newton's method. In the figures, we have only depicted the results of continuation of the low-curvature end of the depicted branches. Branches ending 'in mid air' do not represent the end-point of the branch but where computation was stopped because the magnitude of the curvature was becoming much larger than its minimum value along the branch. Also, the crossing of curves (for example for $\tau = 0.28$ in figure 9*a*) does not have a special meaning and the intersection simply describes two different waves with very different profiles for the same τ. In fact, the 'kinks' in the branches for τ a little larger than 0.28 correspond to the 'envelope' of the generalized solitary wave becoming non-monotonic near the centre of the wave, while the tail amplitude remains of finite size.

Observe from the results that for the entire range of τ-values we have tested, there is no s-shaped curve. We simply get a regular sequence of u and n shapes like the case of the fifth-order KdV equation with $\mu = 0$. This is strong numerical evidence that there are no codimension-one lines in the (F, τ)-plane, bifurcating from $F = 1$ for $9/50 < \tau < 1/3$, at which true elevation solitary waves (with zero tail amplitude) occur.

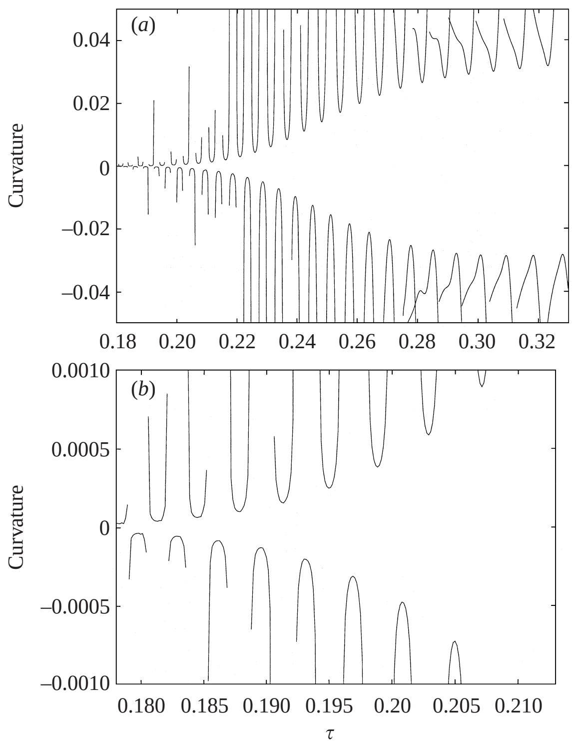

FIGURE 10. (a) A global sweep for $0.18 < \tau < 1/3$ of the small-curvature end of the succession of u- and n-shaped curves for $F = 1.02$ and $L = 98.33$, computed with $N = 135$. Note that no s-shaped curves are found and consequently (as illustrated by the zoom in (b) the minimum tail amplitude is bounded away from zero.

5. Conclusion

Elevation solitary waves do not exist. This is not a proof, but the evidence would appear compelling. At first sight, this conclusion would appear to contradict the results in Vanden-Broeck (1991) which identified generalized solitary waves for which the amplitude of the ripples appears to be zero within graphical accuracy. A closer examination shows that there is no contradiction, since a blow-up of the far-field solution in figure 2(c) of Vanden-Broeck (1991) reveals oscillation on a scale $\sim 10^{-6}$. Note that those results were for fixed $\tau = 0.24$ and, most significantly given the results presented here, a very small F-value of 1.000358. Note that the asymptotics of Yang & Akylas (1996) also support the conclusions of the present paper. Most significantly, we have suggested a new, more reliable numerical test of whether the tail amplitude is ever zero, namely to vary τ for fixed F and L and to assess the topological structure of the ensuing branches of solutions of generalized solitary waves. We have found that the answer is then negative, at least for the τ-values for which the minimum tail amplitude is bigger than numerical precision at the fixed Froude number we chose.

It should be noted that for air–water (for which $T \approx 73$ and $g \approx 9.81$ in units of cm, g and s) $\tau = 0.24$ corresponds to $H \approx 6$ mm. For such depths, viscosity is not irrelevant (Benjamin 1982) and a factor of 10^{-6} in an inviscid model appears insignificant. For smaller values of τ (larger H) the effect of viscosity is less significant, but as we have shown, the minimum tail amplitude decreases for fixed F. Hence, realistically, whether the tail amplitude actually vanishes in the inviscid model does not seem to be physically relevant to everyday flows. Nevertheless, this question has proved to be a historically important one in the theory of gravity–capillary water waves, and we believe our results (based on the topological structure) represent the first categorical piece of numerical evidence that true solitary waves of elevation do not exist for a large range of τ-values.

The authors would like to thank Mark Groves (University of Loughborough) for his key insights at the early stages of this work. The work of ARC is supported by the UK EPSRC with whom he holds an Advanced Fellowship. The work of J.-M. VdB is supported by the UK Leverhulme Trust.

REFERENCES

AKYLAS, T. & GRIMSHAW, R. 1992 Solitary internal waves with oscillatory tails. *J. Fluid Mech.* **242**, 279–298.

AMICK, C. J. & KIRCHGASSNER, K. 1989 A theory of solitary water-waves in the presence of surface tension. *Arch. Rat. Mech. Anal.*

AMICK, C. J. & MCLEOD, J. B. 1991 A singular perturbation problem in water-waves. *Stability Appl. Anal. Continuous Media* **1**, 127–148.

AMICK, C. J. & TOLAND, J. F. 1992 Global uniqueness of homoclinic orbits for a class of 4th order equations. *Z. Angew. Math. Phys.* **43**, 591–597.

BEALE, T. J. 1991 Solitary water waves with capillary ripples at infinity. *Commun. Pure Appl. Maths* **64**, 211–257.

BENJAMIN, T. 1982 The solitary wave with surface tension. *Q. Appl. Maths* **40**, 231–234.

BRIDGES, T. & DERKS, G. 1999 Linear stability of solitary wave solutions of the Kawahara equation and its generalizations. Preprint, Dept. of Maths. and Stats., Univ. of Surrey, Guildford.

BUFFONI, B., CHAMPNEYS, A. R. & TOLAND, J. F. 1996 Bifurcation and coalescence of a plethora of homoclinic orbits for a Hamiltonian system. *J. Dyn. Diffl Equat.* **8**, 221–281.

BUFFONI, B., GROVES, M. D. & TOLAND, J. F. 1996 A plethora of solitary gravity-capillary water waves with nearly critical bond and froude numbers. *Phil. Trans. R. Soc. Lond.* A **354**, 575–607.

BUFFONI, B. & SÉRÉ, E. 1996 A global condition for quasi-random behaviour in a class of conservative systems. *Commun. Pure Appl. Maths* **49**, 285–305.

BURYAK, A. V. & CHAMPNEYS, A. R. 1997 On the stability of solitary wave solutions of the 5th-order KdV equation. *Phys. Lett.* A **233**, 58–62.

CALVO, D., YANG, T. & AKYLAS, T. 2000 On the stability of solitary waves with decaying oscillatory tails. *Proc. R. Soc. Lond.* A **456**, 469–487.

CHAMPNEYS, A. 2000 Codimension-one persistence beyond all orders of homoclinic orbits to singular saddle centres in reversible systems. *Nonlinearity* **14**, 87–112.

CHAMPNEYS, A. R. & GROVES, M. D. 1997 A global investigation of solitary wave solutions to a two-parameter model for water waves. *J. Fluid Mech.* **342**, 199–229.

CHAMPNEYS, A. R. & LORD, G. J. 1997 Computation of homoclinic solutions to periodic orbits in a reduced water-wave problem. *Physica* D **102**, 101–124.

CRAIG, W. & GROVES, M. D. 1994 Hamiltonian long-wave approximations to the water-wave problem. *Wave Motion* **19**, 367–389.

DIAS, F. & KHARIF, C. 1999 Nonlinear gravity and capillary-gravity waves. *Annu. Rev. Fluid Mech.* **31**, 301–346.

DIAS, F. & KUZNETSOV, E. 1999 On the nonlinear stability of solitary wave solutions of the fifth-order Korteweg-de Vries equation. *Phys. Lett.* A **263**, 98–104.

DIAS, F., MENASCE, D. & VANDEN-BROECK, J. 1996 Numerical study of gravity capillary solitary waves. *Eur. J. Mech.* B *Fluids* **15**, 17–36.

DOEDEL, E., CHAMPNEYS, A., FAIRGRIEVE, T., KUZNETSOV, Y., SANDSTEDE, B. & WANG, X. 1997 AUTO97 continuation and bifurcation software for ordinary differential equations. Unpublished: available by anonymous ftp from ftp.cs.concordia.ca, directory pub/doedel/auto.

GRIMSHAW, R. & JOSHI, N. 1995 Weakly nonlocal solitary waves in a singularly perturbed Korteweg-de Vries equation. *SIAM J. Appl. Maths* **55**, 124–135.

HASIMOTO, H. 1970 (in Japanese). *Kagaku* **40**, 401.

HUNTER, J. K. & SCHEURLE, J. 1988 Existence of perturbed solitary wave solutions to a model equation for water-waves. *Physica* D **32**, 253–268.

HUNTER, J. K. & VANDEN-BROECK, J.-M. 1983 Solitary and periodic gravity-capillary waves of finite amplitude. *J. Fluid Mech.* **134**, 205–219.

IOOSS, G. & KIRCHGASSNER, K. 1992 Water waves for small surface tension: an approach via normal form. *Proc. R. Soc. Edin.* A **112**, 267–200.

KAKUTANI, T. & ONO, H. 1969 Weak non-linear hydromagnetic waves in cold collisionless plasma. *J. Phys. Soc. Japan* **26**, 1305–219.

KARPMAN, V. 1994 Stationary solitary waves of the fifth order kdv-type equations. *Phys. Lett.* A **186**, 300–308.

KAWAHARA, T. 1972 Oscillatory solitary waves in dispersive media. *J. Phys. Soc. Japan* **33**, 260–264.

KICHENASSAMY, S. & OLVER, P. J. 1996 Existence and non-existence of solitary wave solutions to higher-order model evolution equations. *SIAM J. Math. Anal.* **23**, 1141–1166.

KORTEWEG, D. & DE VRIES, G. 1895 On the change of the form of long waves advancing in a rectangular canal and a new type of long stationary wave. *Phil. Mag.* **39**, 422–443.

LOMBARDI, E. 2000 *Oscillatory Integrals and Phenomena Beyond all Orders; with Applications to Homolcinic Orbits in Reversible Systems.* Lecture Notes in Mathematics, vol. 1741. Springer.

MICHALLET, H. & DIAS, F. 1999 Numerical study of generalized interfacial solitary waves. *Phys. Fluids* **11**, 1502–1511.

POMEAU, Y., RAMANI, A. & GRAMMATICOS, B. 1988 Structrual stability of the Korteweg-de Vries solitons under a singular perturbation. *Physica* D **31**, 127–134.

STOKER, J. 1957 *Water Waves: the Mathematical Theory with Applications.* Interscience.

SUN, S. 1991 Existence of a generalised solitary wave solution for water waves with poitive bond number less than 1/3. *J. Math. Anal. Appl.* **156**, 471–504.

SUN, S. M. 1998 On the oscillatory tails with arbitrary phase shift for solutions of the perturbed KdV equations. *SIAM J. Appl. Maths* **58**, 1163–1177.

SUN, S. M. 1999 Non-existence of truly solitary waves in water with small surface tension. *Proc. R. Soc. Lond.* A **455**, 2191–2228.

SUN, S. M. & SHEN, M. C. 1993 Exponentially small estimate for the amplitude of capillary ripples of generalised solitary waves', *J. Math. Anal. Appl.* **172**, 533–566.

VANDEN-BROECK, J.-M. 1991 Elevation solitary waves with surface tension. *Phys. Fluids* A **11**, 2659–2663.

VANDEN-BROECK, J.-M. 1997 Weakly nonlocal gravity-capillary solitary waves – comments. *Phys. Fluids* **9**, 245–346.

VANDEN-BROECK, J.-M. & SCHWARTZ, L. 1979 Numerical computation of steep gravity waves in shallow water. *Phys. Fluids* **22**, 1868–1871.

WILTON, J. 1915 On ripples. *Phil. Mag.* **29**, 688–700.

YANG, T. & AKYLAS, T. 1996 Weakly nonlocal gravity-capillary solitary waves. *Phys. Fluids* **8**, 1506–1514.

YANG, T. S. & AKYLAS, T. R. 1997 On asymmetric gravity-capillary solitary waves. *J. Fluid Mech* **330**, 215–232.

ZUFIRIA, J. A. 1987 Symmetry breaking in periodic and solitary gravity-capillary waves on water of finite depth. *J. Fluid Mech.* **184**, 183–206.